

AFRL-ML-WP-TP-2006-459

**ALPHA/BETA HEAT TREATMENT OF
A TITANIUM ALLOY WITH A NON-
UNIFORM MICROSTRUCTURE
(PREPRINT)**



S.L. Semiatin, T.M. Lehner, J.D. Miller, R.D. Doherty, and D.U. Furrer

AUGUST 2006

Approved for public release; distribution is unlimited.

STINFO COPY

If this work is published, ASM International may assert copyright. The U.S. Government is joint author of the work and has the right to use, modify, reproduce, release, perform, display, or disclose the work.

**MATERIALS AND MANUFACTURING DIRECTORATE
AIR FORCE RESEARCH LABORATORY
AIR FORCE MATERIEL COMMAND
WRIGHT-PATTERSON AIR FORCE BASE, OH 45433-7750**

REPORT DOCUMENTATION PAGE

Form Approved
OMB No. 0704-0188

The public reporting burden for this collection of information is estimated to average 1 hour per response, including the time for reviewing instructions, searching existing data sources, gathering and maintaining the data needed, and completing and reviewing the collection of information. Send comments regarding this burden estimate or any other aspect of this collection of information, including suggestions for reducing this burden, to Department of Defense, Washington Headquarters Services, Directorate for Information Operations and Reports (0704-0188), 1215 Jefferson Davis Highway, Suite 1204, Arlington, VA 22202-4302. Respondents should be aware that notwithstanding any other provision of law, no person shall be subject to any penalty for failing to comply with a collection of information if it does not display a currently valid OMB control number. **PLEASE DO NOT RETURN YOUR FORM TO THE ABOVE ADDRESS.**

1. REPORT DATE (DD-MM-YY) August 2006		2. REPORT TYPE Journal Article Preprint		3. DATES COVERED (From - To)	
4. TITLE AND SUBTITLE ALPHA/BETA HEAT TREATMENT OF A TITANIUM ALLOY WITH A NON-UNIFORM MICROSTRUCTURE (PREPRINT)				5a. CONTRACT NUMBER In-house	
				5b. GRANT NUMBER	
				5c. PROGRAM ELEMENT NUMBER N/A	
6. AUTHOR(S) S.L. Semiatin and J.D. Miller (AFRL/MLLMP) T.M. Lehner (University of Dayton) R.D. Doherty (Drexel University) D.U. Furrer (Rolls-Royce Corporation)				5d. PROJECT NUMBER M02R	
				5e. TASK NUMBER 20	
				5f. WORK UNIT NUMBER 00	
7. PERFORMING ORGANIZATION NAME(S) AND ADDRESS(ES) Metals Branch (AFRL/MLLMP) Metals, Ceramics and NDE Division Materials and Manufacturing Directorate Air Force Research Laboratory, Air Force Materiel Command Wright-Patterson AFB, OH 45433-7750 ----- University of Dayton 300 College Park Dayton, OH 45409				8. PERFORMING ORGANIZATION REPORT NUMBER AFRL-ML-WP-TP-2006-459	
9. SPONSORING/MONITORING AGENCY NAME(S) AND ADDRESS(ES) Materials and Manufacturing Directorate Air Force Research Laboratory Air Force Materiel Command Wright-Patterson AFB, OH 45433-7750				10. SPONSORING/MONITORING AGENCY ACRONYM(S) AFRL-ML-WP	
				11. SPONSORING/MONITORING AGENCY REPORT NUMBER(S) AFRL-ML-WP-TP-2006-459	
12. DISTRIBUTION/AVAILABILITY STATEMENT Approved for public release; distribution is unlimited.					
13. SUPPLEMENTARY NOTES If this work is published, ASM International may assert copyright. The U.S. Government is joint author of the work and has the right to use, modify, reproduce, release, perform, display, or disclose the work. Journal article submitted to Metallurgical and Materials Transactions, published by ASM International. PAO Case Number: AFRL/WS 06-2087, 28 Aug 2006.					
14. ABSTRACT The effect of alpha/beta solution temperature and cooling rate on the evolution of microstructure during the heat treatment of Ti-6Al-2Sn-4Zr-2Mo-0.1Si (Ti6242Si) with a partially-spheroidized starting microstructure of equiaxed + remnant lamellar alpha was established. Experiments comprising induction heating to a peak temperature of 971 or 982 °C followed by cooling at a rate of 11 or 42 °C/min revealed that the volume fraction of the equiaxed alpha grew much more rapidly than the lamellar constituent. These results were explained semi-quantitatively using simple diffusion analyses of the growth of either spherical or elliptical particles, taking into account the soft-impingement of the concentration fields. Despite the much lower diffusivity of molybdenum, which appears to control the growth of primary alpha in Ti6242Si, the similarity of the overall kinetics compared to those measured previously for Ti-6Al-4V was explained on the basis of the higher supersaturations developed during cooldown in the present alloy.					
15. SUBJECT TERMS Alpha/beta solution, equiaxed, supersaturations, soft-impingement					
16. SECURITY CLASSIFICATION OF:			17. LIMITATION OF ABSTRACT: SAR	18. NUMBER OF PAGES 46	19a. NAME OF RESPONSIBLE PERSON (Monitor) Sheldon L. Semiatin 19b. TELEPHONE NUMBER (Include Area Code) N/A
a. REPORT Unclassified	b. ABSTRACT Unclassified	c. THIS PAGE Unclassified			

ALPHA/BETA HEAT TREATMENT OF A TITANIUM ALLOY WITH A NON-UNIFORM MICROSTRUCTURE

S.L. Semiatin, T.M. Lehner*, J.D. Miller, R.D. Doherty**, and D.U. Furrer[§]

Air Force Research Laboratory, Materials and Manufacturing Directorate,
AFRL/MLLM, Wright-Patterson Air Force Base, OH 45433

*University of Dayton, 300 College Park, Dayton, OH 45409

**Department of Materials Science and Engineering, Drexel University,
Philadelphia, PA 19104

[§]Rolls-Royce Corporation, P.O. Box 420, Indianapolis, IN 46206

ABSTRACT

The effect of alpha/beta solution temperature and cooling rate on the evolution of microstructure during the heat treatment of Ti-6Al-2Sn-4Zr-2Mo-0.1Si (Ti6242Si) with a partially-spheroidized starting microstructure of equiaxed + remnant lamellar alpha was established. Experiments comprising induction heating to a peak temperature of 971 or 982°C followed by cooling at a rate of 11 or 42°C/min revealed that the volume fraction of the equiaxed alpha grew much more rapidly than the lamellar constituent. These results were explained semi-quantitatively using simple diffusion analyses of the growth of either spherical or elliptical particles, taking into account the soft-impingement of the concentration fields. Despite the much lower diffusivity of molybdenum, which appears to control the growth of primary alpha in Ti6242Si, the similarity of the overall kinetics compared to those measured previously for Ti-6Al-4V was explained on the basis of the higher supersaturations developed during cooldown in the present alloy.

I. INTRODUCTION

The conversion of large ingots of alpha/beta titanium alloys into wrought mill products is very challenging, typically comprising numerous hot working and heat treatment steps ^[1]. Following casting, initial thermomechanical processing (TMP) is usually conducted in the high-temperature, beta phase field in order to produce a recrystallized beta-grain microstructure. The objective of subsequent TMP below the beta transus (temperature below which beta \rightarrow alpha + beta) is to breakdown the colony-alpha structure (developed during cooling following beta processing) into a fine and uniform equiaxed-alpha morphology. Such spheroidization (or globularization, as it is known in industry) occurs during both deformation and intermediate or final heat treatment. Previous research has shown that dynamic spheroidization (i.e., that during deformation) requires strains in excess of those that can be readily imposed for commercial products ^[2]. Thus, static spheroidization (during subsequent heat treatment), in which remnant alpha lamellae undergo boundary splitting and termination migration ^[3-5], is very important to obtain a uniform, wrought, final microstructure.

The time required to complete the static spheroidization of a remnant alpha platelet of diameter d_α and thickness t_α has been shown to depend on its aspect ratio (d_α/t_α), t_α^3 , and $1/D_\beta$, in which D_β denotes the diffusivity through the beta matrix of the rate-limiting solute ^[6]. For a given platelet aspect ratio and thickness, therefore, it can be concluded that alloys with slow-diffusing solutes may require substantially longer (and commercially unfeasible) times to complete spheroidization during heat treatment. In such instances, remnant alpha

platelets, known as spaghetti alpha, may be retained in mill products and persist during secondary processes such as part forging, plate rolling, and final alpha/beta heat treatment. Depending on the thickness of the lamellae and the scale of the remnant colonies, strength, ductility, and fatigue performance may be adversely affected [6-8].

The objective of the present work was twofold - first, to determine how partially-spheroidized microstructures evolve during final alpha/beta heat treatment and thus to establish the impact of remnant lamellae or lamellar colonies on final microstructure and, second, to extend a previous model for the heat treatment of Ti-6Al-4V (Ti64) [9] to an alloy with a solute element whose diffusivity in beta titanium is considerably slower than aluminum or vanadium. These goals were met via a series of induction heat treatments and accompanying diffusion analyses using Ti-6Al-2Sn-4Zr-2Mo-0.1Si (Ti6242Si) as the program material.

II. MATERIALS AND EXPERIMENTAL PROCEDURES

A. *Materials*

The principal material used in the present work was received as a 300-mm-diameter billet of Ti6242Si with a measured composition (in weight percent) of 6.11 aluminum, 2.0 tin, 4.12 zirconium, 1.96 molybdenum, 0.09 silicon, 0.02 iron, 0.135 oxygen, 0.007 carbon, 0.0039 hydrogen, <0.0020 nitrogen, the balance being titanium. The beta-transus temperature T_{β} was determined via a series of heat treatments to be 1000°C. The as-received, room-temperature microstructure comprised a mixture of equiaxed and lamellar (primary) alpha and

a matrix of very fine secondary alpha (Figure 1). At typical alpha/beta heat treatment temperatures, the matrix would be single-phase beta.

All of the Ti6242Si material used in the present work was extracted from a location lying 100 mm from the center of the billet. To determine the beta-approach curve (Figure 2a) and the composition of the alpha and beta phases (Figure 2b) for diffusion analyses, a number of samples were given selected heat treatments at various temperatures for times ranging from 24 h (high temperatures) to 72 hours (lower temperatures) followed by water quenching in each instance. The beta approach curve (i.e., plot of volume fraction of beta as a function of temperature) was determined by image analysis on backscattered electron images (BEI) in a scanning electron microscope (SEM) using FoveaPro™ software. In such images, alpha appears dark because of its lower atomic number, and beta appears white. In samples water quenched from various temperatures, martensitic alpha, which appears gray and lath-like, forms from the metastable beta. The compositions of the individual phases at the particular heat treatment temperatures were determined via wavelength dispersive spectroscopy (WDS) in a JEOL Superprobe 733.

Diffusion-couple samples were fabricated to estimate the diffusivity of molybdenum in beta titanium for use in the diffusion analysis of the growth of primary alpha during cooling following solution heat treatment in the alpha + beta phase field. The materials for these samples were made via non-consumable arc melting of buttons. The nominal compositions (in weight percent) of the buttons were A – Ti-4Al-2Sn-5Zr-5Mo-0.1Si and B – Ti-4Al-2Sn-5Zr-8Mo-0.1Si. Couples

were fabricated as in Reference 10 and heat treated at 955°C for 72 h. Following heat treatment, the diffusion couple was sectioned and metallographically prepared for measurement of the concentration profile via WDS (in a Cameca SX 100 electron microprobe). Data reduction was performed as was done previously^[10] to determine the desired diffusivity values.

B. Induction Heat Treatments

To establish the evolution of microstructure during typical alpha/beta heat treatments, 10-mm-diameter x 90-mm-length bars were machined from the $r = 100$ mm location in the Ti6242Si billet and subjected to a variety of induction-heating cycles using a 7.5 kW, 80-200 kHz solid-state power supply manufactured by Ameritherm, Inc. (Scottsville, NY). Prior to heat treatment, a type-K thermocouple was attached to each sample at the mid-length, mid-diameter position to monitor and control the temperature. During each test, the sample was heated to a peak temperature (T_p) in approximately 10 minutes, soaked at temperature for 30 minutes, cooled at a constant rate, and water quenched (by dropping into a quench tank) after reaching a pre-specified temperature. Peak temperatures of 971 or 982°C were chosen to provide approximately 13 or 25 pct. alpha during solution treatment. Cooling rates of 11 or 42°C/min (20 or 75°F/min) were used based on earlier work for Ti64^[9]. The desired cooling rate was achieved using the control thermocouple and a temperature controller which turned the induction power off and on as needed. The highest cooling rate examined previously for Ti64 (194°C/min)^[9] was not used in the present work because of the limited alpha growth found at this rate

for the previous alloy, and the fact that the present material contained a solute (Mo) which diffuses through beta titanium much more slowly than either aluminum or vanadium ^[11]. Selected heat treatments for each combination of peak temperature and cooling rate were run in duplicate or triplicate.

Following heat treatment, each sample was sectioned at the mid-length location (at which the thermocouple had been located) and prepared metallographically using standard techniques. Heat-treated microstructures were characterized via BEI (at magnifications between 500 and 1000X) near the mid-diameter position to document the growth of the equiaxed and lamellar alpha and the decomposition of the beta matrix during each heat treatment. Quantitative image analysis was conducted on 3-5 micrographs for each sample to determine the volume fractions of equiaxed and lamellar *primary* alpha (i.e., alpha which grew from the constituents present at T_p) and thus obtain data for the calibration of diffusion models. An aspect ratio of 2:1 was used to differentiate the equiaxed from the lamellar alpha. Because of the complexity of the microstructures that were developed, hand painting was necessary prior to image analysis. Although somewhat tedious, this approach was necessitated by the presence of beta-decomposition products (fine secondary-alpha platelets and grain-boundary alpha) which nucleated during cooling. These features could not be subtracted from electronic images using automated techniques. Repeated measurements showed that errors were approximately ± 1 volume pct. for each constituent *in a given micrograph*. Because of the non-uniformity of microstructure, the variation from one micrograph to another was greater, as will be shown in Section IV.

III. MODELING APPROACH

The growth of primary-alpha constituents with an equiaxed or lamellar morphology during cooling was modeled using diffusion analyses from the literature. These analyses and corresponding input data are summarized in this section.

A. Growth of Equiaxed Alpha

As in previous work for Ti64^[9], the growth of equiaxed primary alpha was modeled using the exact solution of Carslaw and Jaeger^[12] and Aaron, et al.^[13] for a spherical particle in a supersaturated matrix:

$$R(t) = 2\lambda(Dt)^{1/2}, \quad (1)$$

in which $R(t)$ is the particle radius as a function of time t , D is the diffusion coefficient, and λ denotes the growth-rate parameter. For the present work involving heat treatments consisting of continuous cooling, the differential form of Equation (1) was used, viz.,

$$dR/dt = 2\lambda^2 D/R. \quad (2)$$

In Equations (1) and (2), the parameter λ takes the place of the supersaturation Ω found in the well-known “constant-radius” solution:

$$\Omega = (C_M - C_I)/(C_P - C_I). \quad (3)$$

Here, C_M , C_I , and C_P represent the compositions of the matrix far from the matrix-particle interface, the matrix at the matrix-particle interface, and the particle at the matrix-particle interface, respectively. For a diffusion-controlled reaction, C_I and C_P correspond to the equilibrium matrix and particle compositions, respectively.

The quantities λ and Ω are related by the following expression:

$$\{\lambda^2 \exp(\lambda^2)\} \cdot [(\exp(-\lambda^2)) - (\lambda\pi^{1/2}\text{erfc}(\lambda))] = \Omega/2 . \quad (4)$$

Equation (4) is not readily inverted to obtain λ as a function of Ω . In the present work, for which many calculations were required, the ‘Solver’ tool of Microsoft Excel was found to be indispensable in determining $\lambda(\Omega)$.

The effect of soft impingement on the ‘far-field’ matrix composition C_M was taken into account using the usual approximation (derived from mass balance considerations ^[14]) which implicitly assumes a uniform solute concentration in both the particle and the matrix, viz.,

$$C_M = (C_o - f_\alpha C_\alpha)/(1 - f_\alpha) , \quad (5)$$

in which C_o and f_α denote the overall alloy composition and the volume fraction of the precipitate/particle phase (primary alpha in the present work), respectively. Because the composition of the alpha phase shows very little variation with temperature (Figure 2b), the particle composition (C_α) and C_P are equivalent and constant.

The application of Equation (5) to describe soft impingement implies a neglect of the precise solute concentration profile in the region immediately adjacent to the alpha particle. In turn, this assumption leads to an *underestimation* of the supersaturation (for cases involving solute diffusion both toward as well as away from the alpha particle). Nevertheless, approximate model calculations with appropriately higher supersaturations suggested that the use of Equation (5) results in a *maximum* under-prediction of the final volume fraction of primary alpha (at 700°C) of approximately 0.5 to 1.5 volume percent, or a value comparable to or less than the accuracy which could be measured experimentally. More detailed phase-field calculations for the growth of primary

alpha during the heat treatment of Ti-6Al-4V ^[15] corroborated this conclusion. The phase-field calculations for Ti-6Al-4V also confirmed that the Carslaw and Jaeger/Aaron, et al. solution ^[12, 13], which is formally applicable to precipitate growth under *isothermal* heat-treatment conditions, provides reasonable estimates of the growth of primary alpha under *non-isothermal* (cooling) conditions for which the shape of the concentration profile changes continuously due to factors such as the decrease of diffusivity with decreasing temperature.

The solution of Equation (2) subject to the soft impingement criterion (Equation (5)) was accomplished using Microsoft Excel spreadsheets for each of the cooling rates employed in the experimental work. The output of the calculations included the particle radius and supersaturation as a function of temperature. The particle radius was converted to volume fraction using the following expression:

$$f_{\alpha} = f_{\alpha 0} (R/R_0)^3 \quad . \quad (6)$$

Here, $f_{\alpha 0}$ and R_0 are the initial volume fraction and particle radius, respectively.

B. Growth of Lamellar Alpha

The growth behavior of remnant lamellar alpha was modeled in a manner similar to that for equiaxed alpha. In this case, remnant lamellae were approximated as being ellipsoidal.[†] The diffusion solution for the growth of an ellipsoidal particle (formed by rotating an ellipse about its *minor axis*), whose aspect ratio (denoted as A) is assumed to remain constant, ^[16-19] was used as an approximation in the present work, i.e.,

[†] Model calculations based on the diffusional thickening of a semi-infinite plate ^[13] were also performed, but yielded predictions inferior to those from the ellipsoidal-particle analysis.

$$Y = 2A(\beta Dt)^{1/2} \quad X = 2(\beta Dt)^{1/2} \quad . \quad (7)$$

In Equation (7), $2Y$ and $2X$ denote the lengths of the major and minor axes of the ellipse, respectively, and the growth-rate parameter β is related to the supersaturation Ω by the following relation:

$$\Omega = [\exp(\beta)] [\beta^{3/2} A^2] \int_{u=\beta}^{u=\infty} \frac{[\exp(-u)] du}{\{\beta(A^2 - 1) + u\} u^{1/2}} \quad . \quad (8)$$

Equation (8) is not readily inverted to obtain $\beta(\Omega)$. Hence, a Microsoft Visual Basic program was written to determine this dependence.

Using Equation (7), the time rate of change of the volume ($V_e = (4/3)\pi Y^2 X$) of the ellipsoidal particle is readily determined to be the following:

$$\frac{dV_e}{dt} = 8\pi A^2 \beta D X \quad . \quad (9)$$

To simplify the spreadsheet calculations for lamellar alpha (i.e., those associated with inverting Equation (8) to obtain $\beta(\Omega)$), the growth rate given by Equation (9) was converted to an expression for the growth of an equivalent spherical particle of radius R_{eff} . The required expression was derived using Equation (1) and the relation for the volume of a sphere ($V_s = (4/3)\pi r^3$) to obtain the volumetric rate of growth for a sphere, dV_s/dt :

$$\frac{dV_s}{dt} = 8\pi \lambda^2 D R_{eff} \quad . \quad (10)$$

Combining Equations (9) and (10), R_{eff} is thus

$$R_{eff} = (A^2 \beta / \lambda^2) X \quad . \quad (11)$$

As will be discussed in Section IV, the *average* aspect ratio of the lamellar plates in the Ti6242Si program alloy was ~ 3.6 . For $A = 3.6$, the numerical

solution of Equations (4) and (8) shows that $\beta/\lambda^2 \approx 0.31 \pm 0.04$ over a wide range of supersaturations (i.e., values of λ^2 between 0 and 4). Thus, Equation (11) indicates that R_{eff} equals approximately $4X$, or twice the lamellar thickness ($2X$). Hence, the volumetric rate of growth of a lamellar platelet is much slower than that of a spherical particle whose diameter is equal to the platelet thickness.

The definition of R_{eff} allowed the calculation of the growth of the lamellar phase in a manner equivalent to that described in Section III.A with soft impingement taken into account in a similar fashion.

C. Model Calculations and Input Data

Two sets of model calculations were performed to gauge the growth of the mixed equiaxed-lamellar microstructure. In the first set, it was assumed that the equiaxed and lamellar alpha were uniformly distributed throughout the beta matrix. Thus, the supersaturation seen by each constituent was taken to be identical. In this case, the growth of the two morphologies was coupled, and the instantaneous supersaturation was affected by their respective growth rates. For the second set of calculations, it was assumed that the equiaxed and lamellar phases were treated as isolated patches in each of which a different supersaturation developed. Hence, the rate of growth of each morphology was calculated separately. The total volume fraction of alpha as a function of time (and temperature) during cooling was then estimated as a weighted sum of the two calculated volume fractions. Each weighting factor was equal to the quotient of the initial volume fraction of the particular constituent divided by the total initial volume fraction of primary alpha.

The input data for the diffusion analyses consisted of the equilibrium phase compositions as a function of temperature (Figure 2b), the initial size and volume fraction of the equiaxed-alpha and the lamellar-alpha constituents at the peak temperature (Table I), and the pertinent diffusivity D . Because of the globular nature of the equiaxed-alpha phase, the initial particle radius for this constituent was taken to be the radius of a circle whose area was equal to the average area of the globular particles determined from micrographs taken on 2D sections. On the other hand, an intercept method was used to determine the platelet thickness t_α because it is not possible to determine the angle between the platelet normal and the plane of view without doing serial sectioning. The relation between the actual platelet thickness t_α and the average value of the inverse intercept length ($1/\Lambda$) of a series of lines set at arbitrary angles over the micrograph is the following [20]:

$$t_\alpha = \frac{1}{1.5(1/\Lambda)_{\text{mean}}} , \quad (12)$$

Because of the equiaxed nature (in the plan view) of the lamellae [4], their diameter was taken to be simply the average length measured from BEI micrographs.

With respect to the pertinent value of D to use in the analysis, it was hypothesized that the solute for which the values of $\lambda^2 D$ (or βD) were least would control growth, as suggested by Equations (2) and (9). The maximum supersaturation of aluminum or molybdenum that would be developed during rapid cooling from temperatures just below the beta transus was thus estimated

from Figure 2b (for Mo) and the data in Reference 9 (for Al). The values of diffusivity in Reference 10 (for Al) and impurity diffusion in Reference 11 (for Mo) in conjunction with the estimated supersaturations confirmed that molybdenum diffusion through the beta matrix would indeed most likely limit the growth of alpha during cooling. The specific dependence of D_{Mo}^{β} on absolute temperature (T(K)) was based on the results from Reference 11 and by a “calibration factor” (CF) determined from the present diffusion-couple experiments., i.e.,

$$D_{Mo}^{\beta} (\mu\text{m}^2/\text{s}) = \text{CF} \times 70000 \exp(-18520/T(\text{K})) . \quad (13)$$

The value of D_{Mo}^{β} determined from the experiments was $0.015 \mu\text{m}^2/\text{s}$ at 955°C , thus indicating that $\text{CF} \approx 0.75$. A comparison of the present and previous ^[10] results indicates that the diffusivity of molybdenum in beta titanium (with solutes of Al, Sn, Zr, and Si) is $\sim 1/6$ of those for aluminum and vanadium (which are comparable to each other).

IV. RESULTS AND DISCUSSION

The principal results from this work comprised measurements of the growth of primary alpha during cooling, diffusion-model calculations to describe the observed behavior, and a comparison of the alpha/beta heat treatment response of Ti6242Si with previous observations and calculations for Ti64 ^[9].

A. Heat Treatment Behavior of Ti6242Si

Typical microstructures developed during cooling at a rate ($\dot{\theta}$) of 11 or $42^{\circ}\text{C}/\text{min}$ following solution treatment at 971 or 982°C revealed various aspects of the growth of the primary alpha and, in some cases, decomposition of the beta

matrix to form secondary alpha with a fine platelet morphology. For $T_p = 971^\circ\text{C}$ and $\dot{\theta} = 11^\circ\text{C}/\text{min}$ (Figure 3), primary alpha with both the equiaxed and lamellar morphologies grew essentially epitaxially with very little to no beta-matrix decomposition; i.e., the diameter of the equiaxed particles and the thickness of the lamellar particles increased. The only exception to these observations was the sporadic appearance of a morphological instability of the primary alpha at the interphase interfaces. Examples of such instability are indicated by the arrows in Figures 3c and 3d and are similar to previous findings for the heat treatment of Ti64 [9].

Microstructure evolution for $T_p = 971^\circ\text{C}$ and $\dot{\theta} = 42^\circ\text{C}/\text{min}$ (Figure 4) indicated similar epitaxial growth of primary alpha with both morphologies at high temperatures ($\geq 870^\circ\text{C}$), but noticeable decomposition of the beta matrix at lower temperatures. When the temperature had decreased to $\sim 815^\circ\text{C}$, approximately one-half of the matrix had transformed, whereas it appeared to be fully transformed at 705°C . The cooling rate and temperature dependence of matrix decomposition for Ti6242 was thus similar to that for Ti64 [9].

The effect of cooling rate on microstructure evolution for the higher solution temperature ($T_p = 982^\circ\text{C}$, Figures 5 and 6) was similar to that at the lower peak temperature. The only noticeable difference was that matrix decomposition occurred at somewhat *higher* temperatures for $\dot{\theta} = 42^\circ\text{C}/\text{min}$ (Figure 6 versus Figure 4). This behavior also mirrored previous results for Ti64 concerning the effect of peak temperature and cooling rate on beta-matrix decomposition [9].

Volume-fraction and aspect-ratio measurements for the equiaxed and lamellar primary-alpha constituents quantified the metallographic observations. For each combination of peak temperature and cooling rate, the volume fraction of equiaxed alpha grew substantially faster than that for the lamellar alpha (Figures 7 and 8). Specifically, the equiaxed-alpha volume fraction increased by a factor of ~4 to 5 (lower cooling rate, Figures 7a, 8a) or ~3 to 4 (higher cooling rate, Figures 7b, 8b) between T_p and 705°C. By contrast, the lamellar-alpha volume fraction increased by a factor of approximately 2. This difference in growth rate can be explained qualitatively by the approximately twofold difference in the average radius (R) of the equiaxed-alpha particles and the effective radius (R_{eff}) of the lamellar alpha (Table I) and the fact that the growth rate varies *inversely* to the radius (Equation (2)).

Metallography to determine the width (diameter) and thickness of the lamellar-alpha particles quantified the degree of approximation associated with the assumption of a constant aspect ratio (A) during growth. These results showed a slight variation with temperature during cooling (Figure 9), but the approximation of $A \sim 3.6$ appeared to be reasonable to a first order, especially for higher temperatures ($T \geq 850^\circ\text{C}$) at which most of the diffusional growth had occurred. Specifically, the average value of A was ~ 3.5 or ~ 3.75 for $T_p = 971$ or 982°C , respectively.

The results in Figure 7 for $T_p = 971^\circ\text{C}$ suggested that the volume fraction of lamellar primary alpha passed through a maximum during cooling. This effect may be rationalized to some extent by small decreases in the aspect ratio of

those lamellae whose *initial* aspect ratio was close to the 2:1 threshold used to differentiate the equiaxed and lamellar morphologies. However, the magnitude of the experimental uncertainty associated with the quantitative metallography and the absence of corresponding maxima for the $T_p = 982^\circ\text{C}$ results (Figure 8) precluded a precise explanation for such observations.

B. Model Predictions

Diffusion-model results provided insight into the effect of peak temperature and cooling rate on the growth of primary alpha with the equiaxed and lamellar morphologies. Irrespective of the specific set of process variables, the equiaxed-alpha volume fraction was predicted to grow at a rate several times faster than that for the lamellar-alpha volume fraction (Figures 10 and 11), an effect largely due to the larger *effective* radius of the lamellar alpha. Furthermore, calculations based on the coupled growth of the two constituents (for which the supersaturation was assumed to be the same for both) predicted *faster* growth and *larger* overall final volume fractions for the total alpha than the decoupled case (in which each constituent was assumed to be isolated from the other and hence able to develop its own supersaturation). This effect can be ascribed to the slow growth of the lamellar alpha in the coupled case and the concomitant larger supersaturations developed in the matrix which promote the growth of equiaxed alpha. The high growth rate of the equiaxed alpha in turn reduced the supersaturation that would have been developed around isolated alpha lamellae. Hence, the coupled simulations generally led to larger volume fractions of equiaxed alpha and smaller volume fractions of lamellar alpha than the

decoupled simulations for each combination of peak temperature and cooling rate.

The model predictions quantified the expected effects of cooling rate and peak temperature on the final alpha volume fraction. Irrespective of peak temperature, the slower cooling rate gave rise to predicted total volume fractions that were 10-15 pct. lower than that which would have been achieved under very slow (equilibrium) conditions. The faster cooling rate (42°C/min) was predicted to yield total amounts of primary alpha that were ~25 volume pct. lower than the slower cooling rate. It was also found that the predicted *final* total volume fractions (at 705°C) for the faster cooling rate differed by only ~5 pct for the two different peak temperatures. This value is less than the difference in *initial* volume fractions at the peak temperatures (0.13 at 982°C and 0.25 at 971°C), and can be explained to be a result of several competing effects. Two factors which tended to *reduce* the difference include the smaller initial alpha particle size and higher initial diffusivities for $T_p = 982^\circ\text{C}$. On the other hand, the slightly higher temperature at which secondary alpha started to form for $T_p = 982^\circ\text{C}$ (as suggested by the different volume fractions of transformed beta in the 871°C micrographs in Figures 4 and 6) tended to mitigate the narrowing of the primary-alpha volume-fraction difference for the two peak temperatures.

To validate the modeling approach, the predictions were compared to the experimental data in Figures 7 and 8. Agreement with the measurements was better for the decoupled analysis, most likely because the equiaxed and lamellar morphologies tended to occur in discrete patches in the Ti6242Si program alloy.

Hence, only the decoupled-analysis predictions are plotted in the figures for the sake of clarity. The comparison shows that the correct trends were replicated not only for the total volume fraction of alpha, but also for the separate volume fractions of equiaxed alpha and lamellar alpha. The agreement is very good for the slower cooling rate (Figures 7a and 8a) for which essentially no secondary alpha is formed during cooling and hence the diffusional-growth analysis is very appropriate. For the higher cooling rate ($\dot{\theta} = 42^\circ\text{C}/\text{min}$), the predicted volume fractions of alpha at 705°C were either slightly *less* ($T_p = 971^\circ\text{C}$) or *greater* ($T_p = 982^\circ\text{C}$) than those measured (Figures 7b and 8b). The latter trend is as expected due to the development of secondary alpha and the associated loss of the supersaturation which drives the growth of primary alpha.

The *underprediction* of the volume fraction of alpha for $T_p = 971^\circ\text{C}$, $\dot{\theta} = 42^\circ\text{C}/\text{min}$ may be explainable in the context of the scatter in the experimental measurements, approximations in the models regarding the assumed geometry of the alpha particles (i.e., spherical/elliptical particles) and constancy of the aspect ratio of the lamellae, and, last, errors in the input material data for the models (e.g., diffusivity, phase compositions). For example, use of a somewhat lower aspect ratio (say 3.2 to 3.4, instead of 3.6, as suggested by the data for $T_p = 971^\circ\text{C}$ in Figure 9) would have increased the predicted growth rate of the lamellar alpha to yield predicted final *total* volume fractions of alpha (at 704°C) that are comparable to or slightly higher than those measured; as noted above, predictions higher than the measurements would be expected due to the development of secondary alpha at temperatures $T \leq 870^\circ\text{C}$ (Figure 4). More

detailed analysis of the sensitivity of the model predictions to the aspect ratio/effective radius is thus given in Section IV.C. Nevertheless, the overall agreement between the predictions and measurements is thought to be good in view of the non-uniformity in the Ti6242Si microstructure and difficulties in applying analytical diffusion analyses in such cases.

C. Sensitivity Analysis

A sensitivity analysis, based on the decoupled-solution approach, revealed that the observed variations in aspect ratio (Figure 9) and the assumption of a fixed relation between λ^2 and β have only a small effect on the conclusions drawn in Section IV.B. The key parameter of interest in this analysis was the effective radius of the lamellae (R_{eff}) and its dependence on the lamellar thickness ($2X$) through Equation (11). Lower and upper limits on R_{eff} were determined to be $\sim 3X$ and $\sim 5X$, respectively, based on $A = 3.4$, $\lambda^2/\beta = 0.27$ for the former case and $A = 3.8$, $\lambda^2/\beta = 0.35$ for the latter. Relative to the behavior for the baseline case ($R_{\text{eff}} = 4X$), model predictions for these values of R_{eff} (Figure 12) showed relatively small changes in the predicted growth rate for the lamella- alpha constituent and thus the overall alpha volume fraction as well.

D. Comparison of Ti6242Si and Ti64 Behaviors

The present observations and model predictions for the volume fraction of alpha developed in Ti6242Si during cooling following alpha/beta solution heat treatment showed a striking similarity with previous results for Ti64 with a fully

equiaxed-alpha microstructure. Thus, it is instructive to determine the source of the similarity, especially in view of the low diffusivity of molybdenum which appears to control the diffusional-growth process in Ti6242Si. For this purpose, model calculations were performed for both alloys. In all instances, it was assumed that the initial microstructure was fully equiaxed with an alpha-particle radius of 4 μm . Peak temperatures (969°C for Ti6242Si, 955°C for Ti64) were chosen to provide an initial alpha volume fraction of 0.27. The diffusional growth was assumed to be limited by molybdenum diffusion for Ti6242Si and aluminum diffusion for Ti64 (per the results in Reference 9).

The model calculations did indeed show that comparable volume fractions of alpha were predicted to develop in the two alloys during cooling at both 11 and 42°C/min (Figure 13a). In particular, Ti6242Si was predicted to develop a slightly *larger* or *smaller* volume fraction of alpha at the slower or faster cooling rate, respectively. The source of this similarity was explained on the basis of the supersaturations developed during cooling for the two alloys. This comparison (Figure 13b) shows only a 2-3 fold higher supersaturation (Ω) developed in Ti6242Si. On the other hand, the corresponding values of λ^2 for Ti6242Si were of the order of 5 times as high as those for Ti64 because of the non-linear relation between λ^2 and Ω (Figure 13c). Because the diffusional growth rate is proportional to λ^2 (Equation (2)), it can thus be concluded that the similarity of the volume fractions of alpha developed in the two alloys under similar cooling conditions is due to the fact that the higher levels of λ^2 offset the approximately six-fold lower values of molybdenum diffusivity.

In closing, an examination of the calculated supersaturation values for Ti6242Si (Figure 13b) in light of the microstructure observations (Figures 3-6) suggests that a critical value of Ω (of the order of 0.6) is required for the onset of beta-matrix decomposition. As suggested by previous work for Ti-6Al-4V ^[9], however, a parameter depending on the supersaturation, cooling rate, *and* diffusivity may be more appropriate in quantifying the conditions under which secondary-alpha platelets forms. Research to establish this relationship is currently underway.

V. SUMMARY AND CONCLUSIONS

The alpha/beta heat treatment response of Ti6242Si with a non-uniform microstructure of equiaxed and lamellar alpha was established using a series of induction heat treatments and accompanying diffusion-model calculations. The following conclusions were drawn from this work:

1. The growth of primary alpha with a non-uniform microstructure comprising patches of equiaxed and lamellar alpha can be described by a decoupled diffusion analysis for each of the two morphologies. In such an analysis, the supersaturations which drive the growth of the equiaxed and lamellar phases during cooling develop independently of each other.
2. The diffusion analysis for the lamellar morphology can be reformulated in terms of the growth of spherical particles (with a so-called effective radius) whose volumetric growth is equivalent to that of the lamellae.
3. The diffusion analysis is capable of quantifying the slower volumetric growth rate of lamellar alpha relative to the equiaxed alpha.

4. The similarity of the growth kinetics during cooling of Ti6242Si and Ti64 can be attributed to the combined influence of lower diffusivity of the rate limiting solute (molybdenum) and higher supersaturations that develop for Ti6242Si.

Acknowledgements - This work was conducted as part of the in-house research of the Metals Processing Group of the Air Force Research Laboratory's Materials and Manufacturing Directorate. The support and encouragement of the laboratory management and the Air Force Office of Scientific Research (Dr. J.S. Tiley, program manager) are gratefully acknowledged. The project effort was also partly supported by the Air Force Metals Affordability Initiative program on Microstructure and Mechanical Property Modeling for Wrought Titanium Alloys being led by Ladish Company, Cudahy, WI. Two of the authors were supported under the auspices of Contracts F33615-02-2-5800 (TML) and F33615-99-2-5215, Project LAD-2 (DUF). The assistance of P. Fagin, T. Brown, and T. Goff in conducting the experiments is gratefully acknowledged.

REFERENCES

1. S.L. Semiatin: in *Advances in the Science and Technology of Titanium Alloy Processing*, I. Weiss, R. Srinivasan, P.J. Bania, D. Eylon, and, S.L. Semiatin, eds., TMS, Warrendale, PA, 1997, pp. 3-73.
2. S.L. Semiatin, V. Seetharaman, and I. Weiss: *Materials Science and Engineering*, 1999, vol. A263, pp. 257-271.
3. N. Stefansson, S.L. Semiatin, and D. Eylon: *Metall. and Mater. Trans. A*, 2002, vol. 33A, pp. 3527-3534.
4. N. Stefansson and S.L. Semiatin: *Metall. and Mater. Trans. A*, 2003, vol. 34A, pp. 691-698.
5. S.L. Semiatin, N. Stefansson, and R.D. Doherty: *Metall. and Mater. Trans. A*, 2005, vol. 36A, pp. 1372-1376.
6. S. Suri, S.L. Semiatin, and M.J. Mills: Unpublished research, Air Force Research Laboratory, Wright-Patterson Air Force Base, OH, 2000.
7. G. Luetjering and M. Peters: Report CS-2933, Electric Power Research Institute, Palo Alto, CA, 1983.

8. A.P. Woodfield, M.D. Gorman, R.R. Corderman, J.A. Sutliff, and B. Yamron: in *Titanium '95: Science and Technology*, P.A. Blenkinsop, W.J. Evans, and H.M. Flower, eds., Institute of Materials, London, pp. 1116 – 1123.
9. S.L. Semiatin, S.L. Knisley, P.N. Fagin, F. Zhang, and D.R. Barker: *Metall. and Mater. Trans. A*, 2003, vol. 34A, pp. 2377-2387.
10. S.L. Semiatin, T.M. Brown, T.A. Goff, P.N. Fagin, D.R. Barker, R.E. Turner, J.M. Murry, J.D. Miller, and F. Zhang, *Metall. and Mater. Trans. A*, 2004, vol. 35A, pp. 3015-3018.
11. U. Zwicker: *Titanium and Titanium Alloys*, Springer Verlag, Berlin, 1974.
12. H.S. Carslaw and J.C. Jaeger: *Conduction of Heat in Solids*, Oxford University Press, London, 1959.
13. H.B. Aaron, D. Fainstein, and G.R. Kotler: *J. Appl. Physics*, 1970, vol. 41, pp. 4404-4410.
14. O. Grong and H.R. Shercliff: *Progress in Materials Science*, 2002, vol. 47, pp. 163-282.
15. Y. Wang, N. Ma, Q. Chen, F. Zhang, S.-L. Chen, and A. Chang: *JOM*, 2005, vol. 57, no. 9, pp. 32-39.
16. F.S. Ham: *J. Phys. Chem. Solids*, 1958, vol. 6, pp. 335-351.
17. F.S. Ham: *Q. Appl. Math.*, 1959, vol. 17, pp. 137-145.
18. G. Horvay and J.W. Cahn: *Acta Metall.*, 1961, vol. 9, pp. 695-705.
19. M. Ferrante and R.D. Doherty: *Acta Metall.*, 1979, vol. 27, pp. 1603-1614.
20. H.J.G. Gundersen, T.B. Jensen, and R. Osterby: *J. Microscopy*, 1978, vol. 113, pp. 27-43.

Table I. Ti6242Si Microstructure Characteristics

Temp (°C)	f_{α} Equiaxed	R_{α} (μm) Equiaxed	f_{α} Lamellar	2X (μm) Lamellar	A Lamellar*	R_{eff} (μm) Lamellar**
971	0.16	3.01	0.09	2.87	3.78	5.75
982	0.085	2.56	0.045	2.43	4.76	4.85

* Aspect ratio of lamellae at peak temperature

** $R_{\text{eff}} = 4X$

Figure Captions

- Figure 1. Optical microstructure of as-received Ti6242Si program material.
- Figure 2. Phase equilibria for the Ti6242Si program material: (a) Beta-approach curve and (b) aluminum and molybdenum content in the alpha and beta phases as a function of temperature.
- Figure 3. Microstructures developed in Ti6242Si samples during induction heat treatment comprising soaking at 971°C for 30 min, cooling at a rate of 11°C/min, and water quenching at the temperatures (T_q) indicated.
- Figure 4. Microstructures developed in Ti6242Si samples during induction heat treatment comprising soaking at 971°C for 30 min, cooling at a rate of 42°C/min, and water quenching at the temperatures (T_q) indicated.
- Figure 5. Microstructures developed in Ti6242Si samples during induction heat treatment comprising soaking at 982°C for 30 min, cooling at a rate of 11°C/min, and water quenching at the temperatures (T_q) indicated.
- Figure 6. Microstructures developed in Ti6242Si samples during induction heat treatment comprising soaking at 982°C for 30 min, cooling at a rate of 42°C/min, and water quenching at the temperatures (T_q) indicated.
- Figure 7. Measured variation of the volume fraction of primary equiaxed, lamellar, and total alpha as a function of temperature during cooling from $T_p = 971^\circ\text{C}$ at a rate of (a) 11°C/min or (b) 42°C/min. The measurements (data points, solid lines) are compared to model predictions using the decoupled-solution approach (broken lines).

- Figure 8. Measured variation of the volume fraction of primary equiaxed, lamellar, and total alpha as a function of temperature during cooling from $T_p = 982^\circ\text{C}$ at a rate of (a) $11^\circ\text{C}/\text{min}$ or (b) $42^\circ\text{C}/\text{min}$. The measurements (data points, solid lines) are compared to model predictions using the decoupled-solution approach (broken lines).
- Figure 9. Dependence of aspect (length:thickness) ratio on temperature for remnant alpha lamellae in Ti6242Si during cooling following solution heat treatment.
- Figure 10. Model predictions of the volume fraction of primary alpha as a function of temperature during cooling from a peak temperature equal to 971°C at a rate of (a) $11^\circ\text{C}/\text{min}$ or (b) $42^\circ\text{C}/\text{min}$.
- Figure 11. Model predictions of the volume fraction of primary alpha as a function of temperature during cooling from a peak temperature equal to 982°C at a rate of (a) $11^\circ\text{C}/\text{min}$ or (b) $42^\circ\text{C}/\text{min}$.
- Figure 12. Sensitivity analysis for the growth kinetics of primary alpha assuming $R_{\text{eff}} = 3X, 4X, \text{ or } 5X$ for the two peak temperatures and two cooling rates.
- Figure 13. Comparison of model calculations for the heat-treatment response of Ti6242Si and Ti64, each having an equiaxed microstructure with an alpha particle radius of $4 \mu\text{m}$ and alpha volume fraction of 0.27 at T_p , cooled at either 11 or $42^\circ\text{C}/\text{min}$: (a) Volume fraction of alpha, (b) supersaturation Ω , and (c) λ^2 .

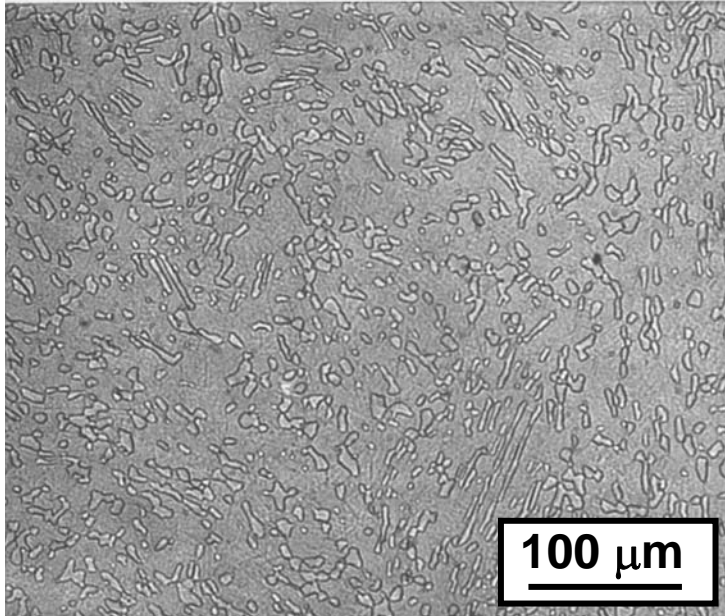


Figure 1. Optical microstructure of as-received Ti6242Si program material.

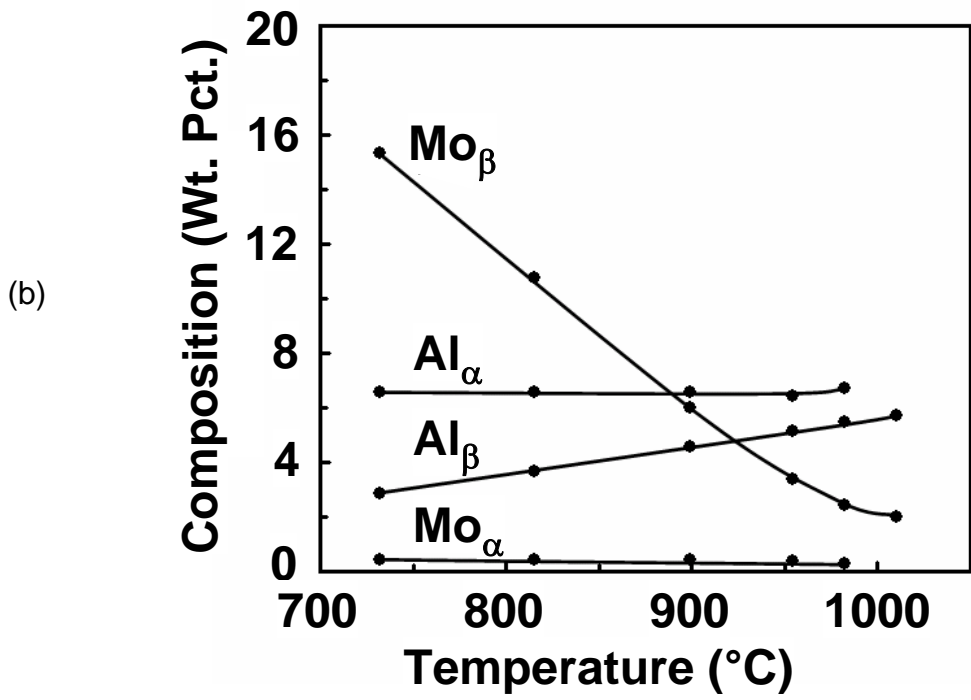
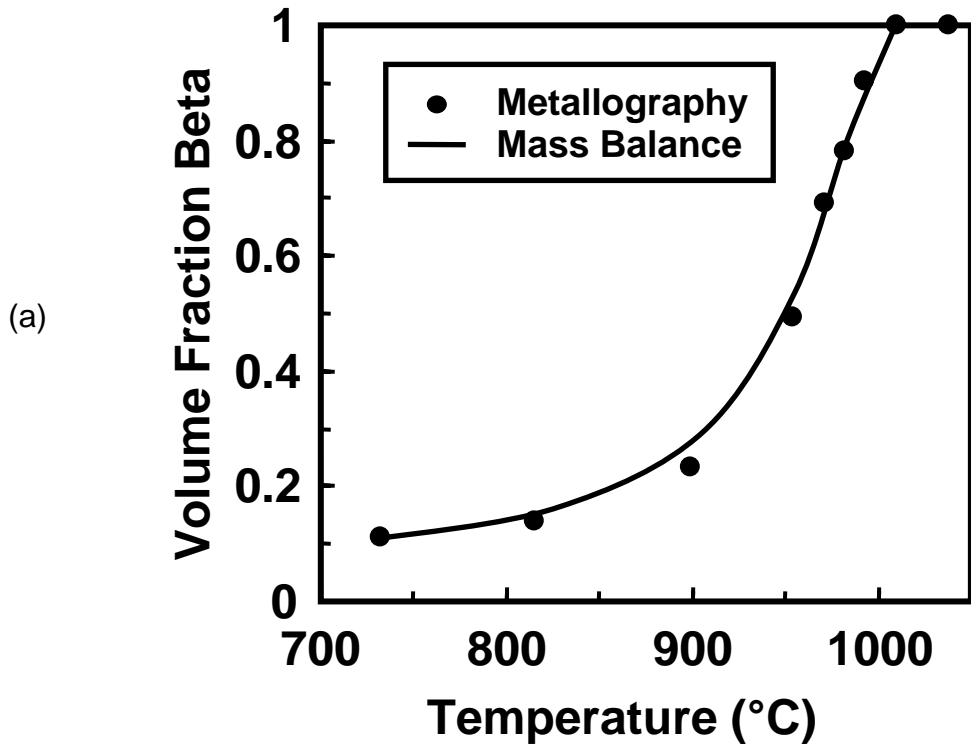


Figure 2. Phase equilibria for the Ti6242Si program material: (a) Beta-approach curve and (b) aluminum and molybdenum content in the alpha and beta phases as a function of temperature.

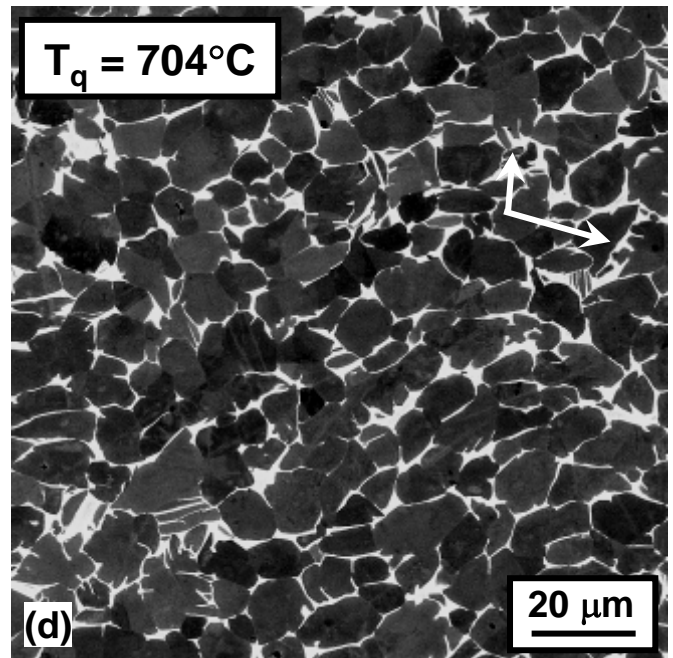
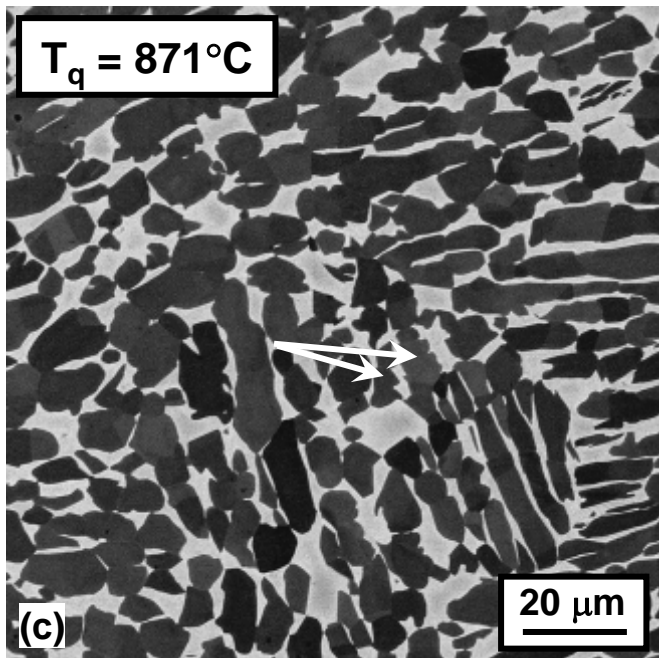
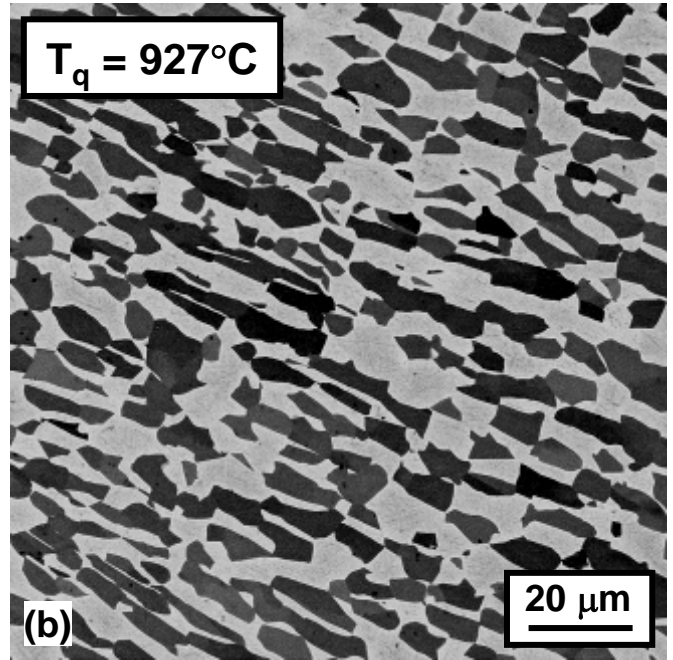
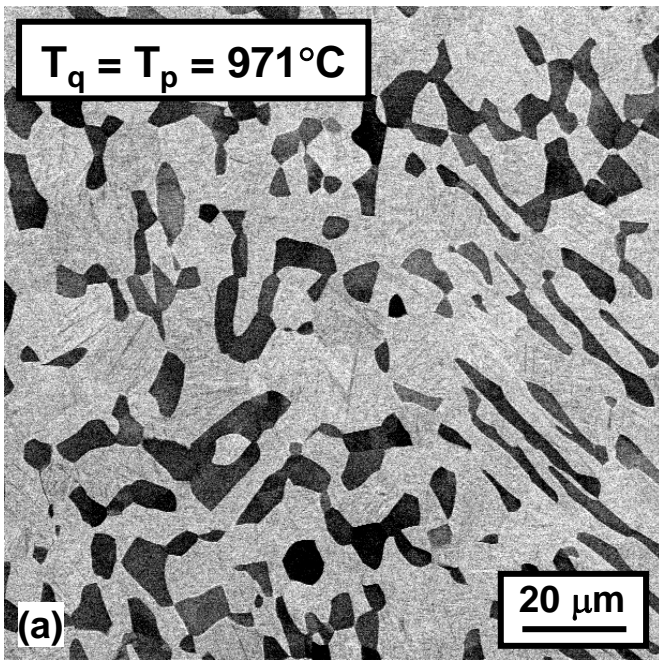


Figure 3. Microstructures developed in Ti6242Si samples during induction heat treatment comprising soaking at 971°C for 30 min, cooling at a rate of $11^\circ\text{C}/\text{min}$, and water quenching at the temperatures (T_q) indicated.

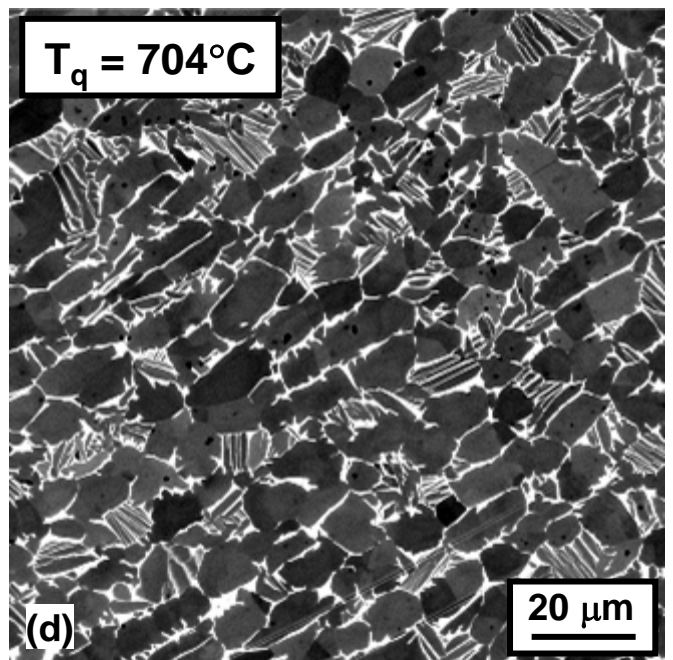
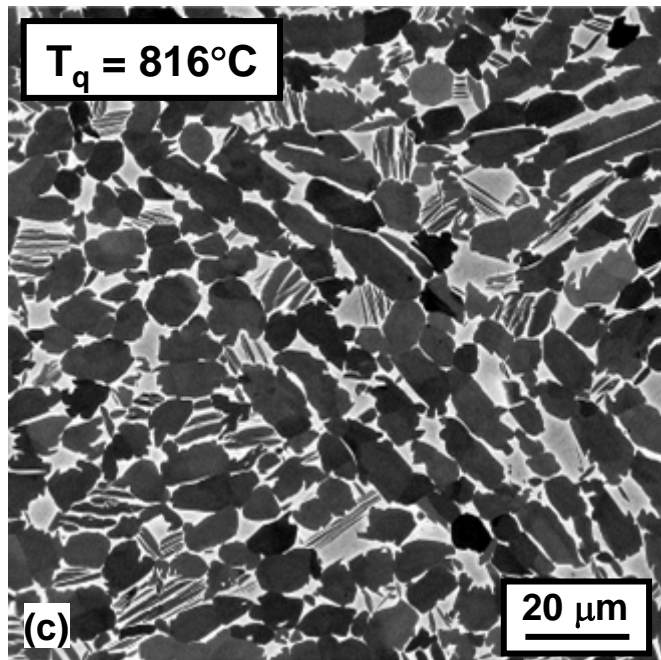
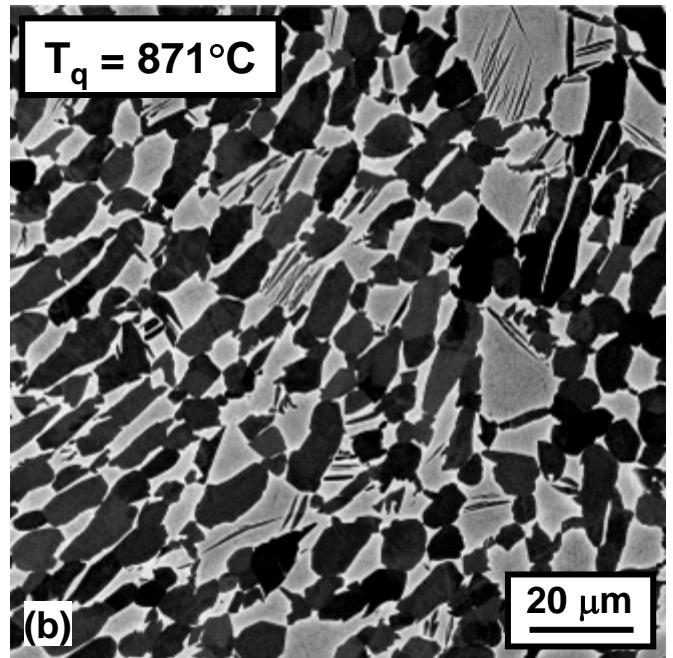
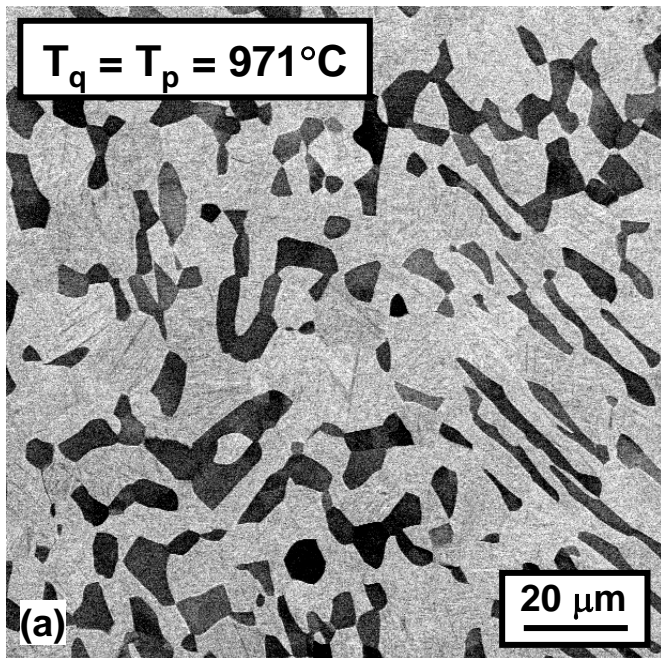


Figure 4. Microstructures developed in Ti6242Si samples during induction heat treatment comprising soaking at 971°C for 30 min, cooling at a rate of $42^\circ\text{C}/\text{min}$, and water quenching at the temperatures (T_q) indicated.

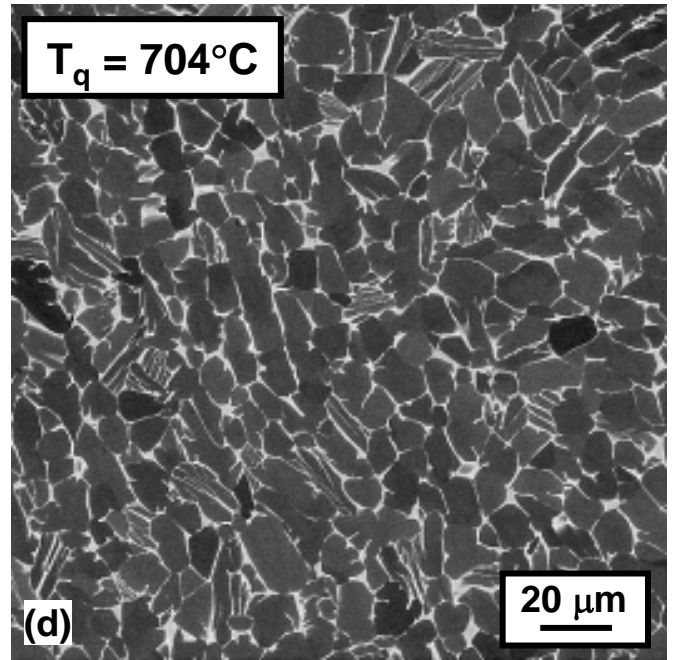
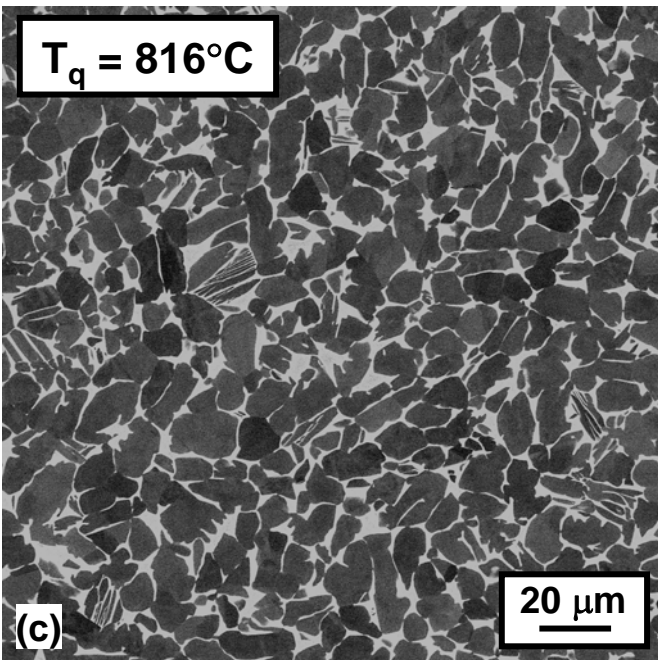
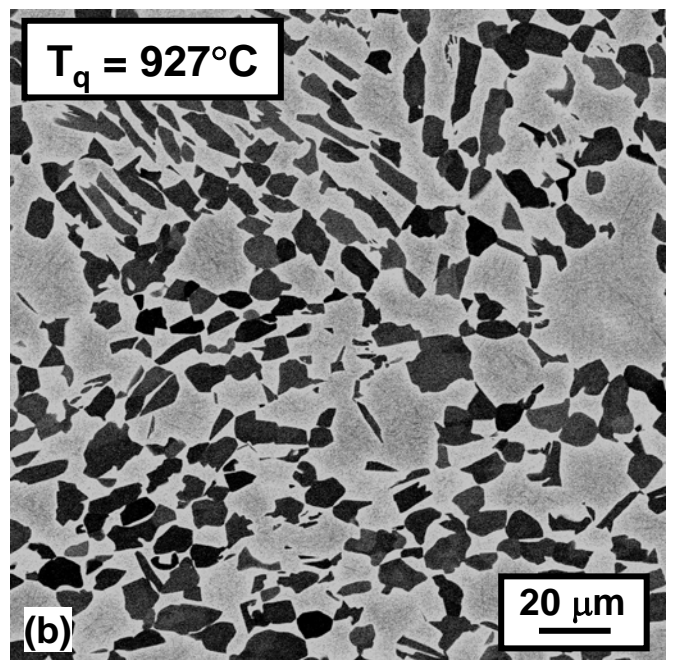
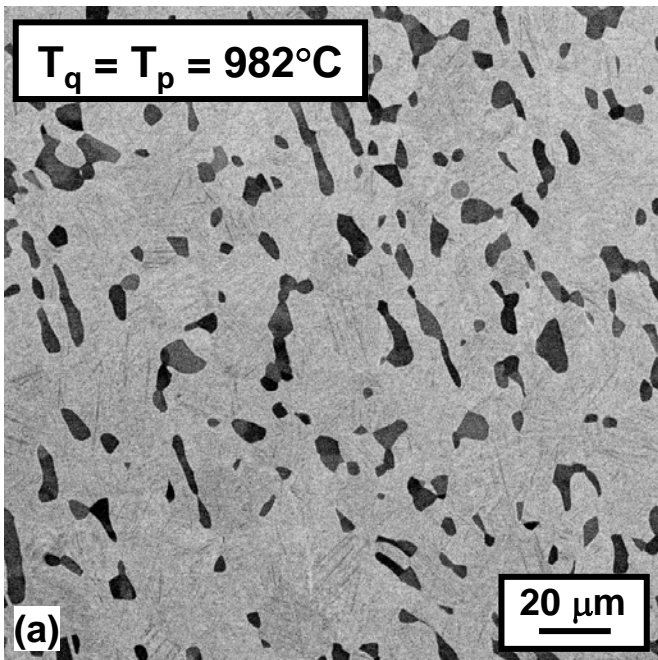


Figure 5. Microstructures developed in Ti6242Si samples during induction heat treatment comprising soaking at 982°C for 30 min, cooling at a rate of $11^\circ\text{C}/\text{min}$, and water quenching at the temperatures (T_q) indicated.

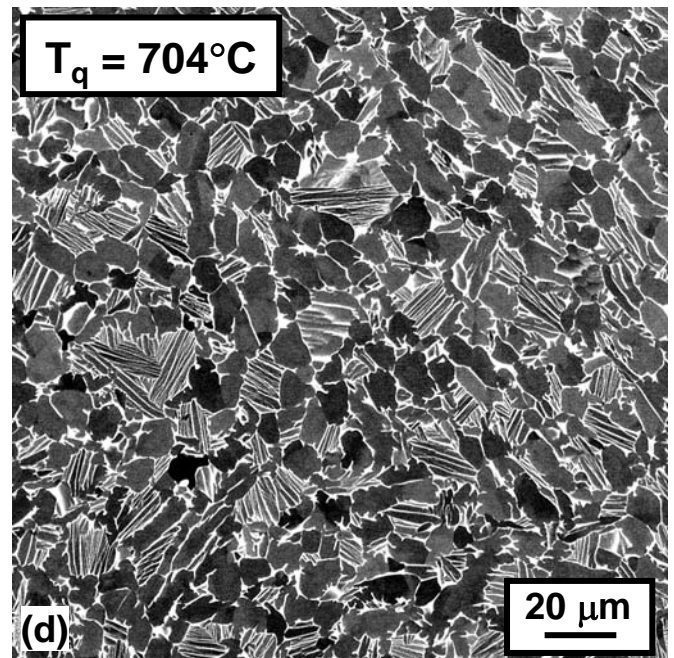
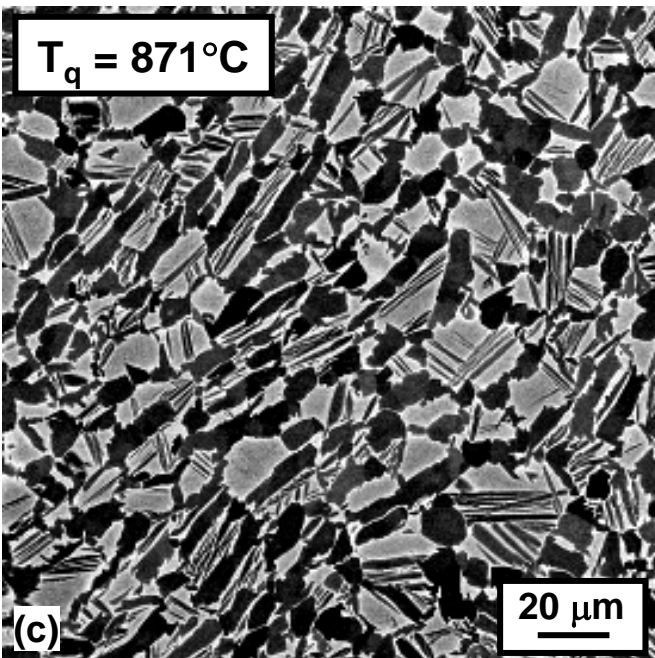
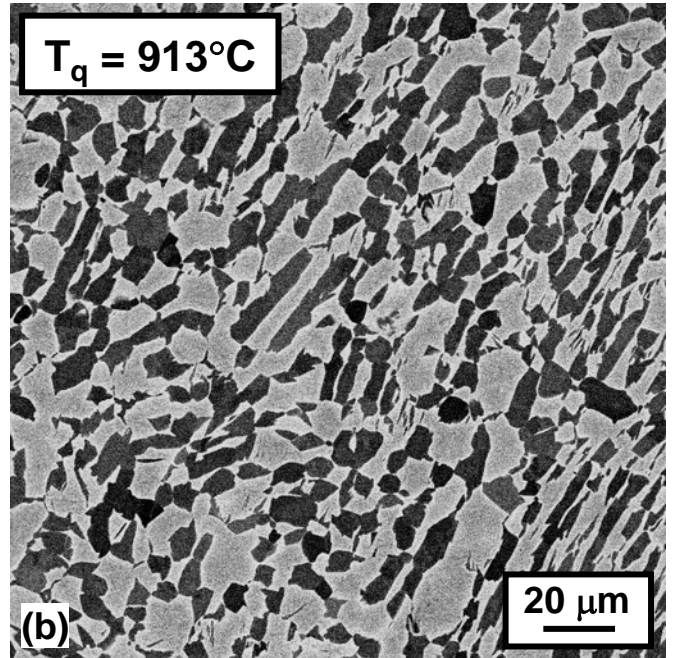
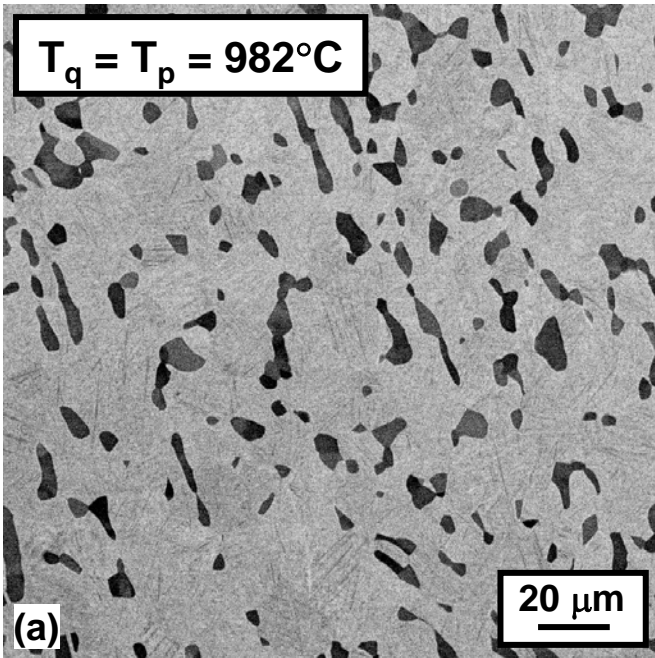


Figure 6. Microstructures developed in Ti6242Si samples during induction heat treatment comprising soaking at 982°C for 30 min, cooling at a rate of $42^\circ\text{C}/\text{min}$, and water quenching at the temperatures (T_q) indicated.

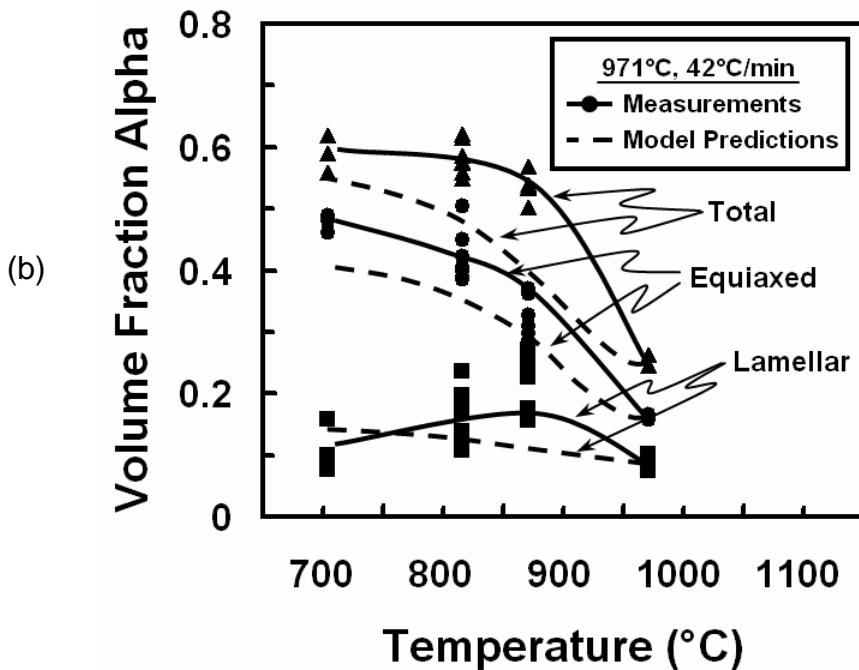
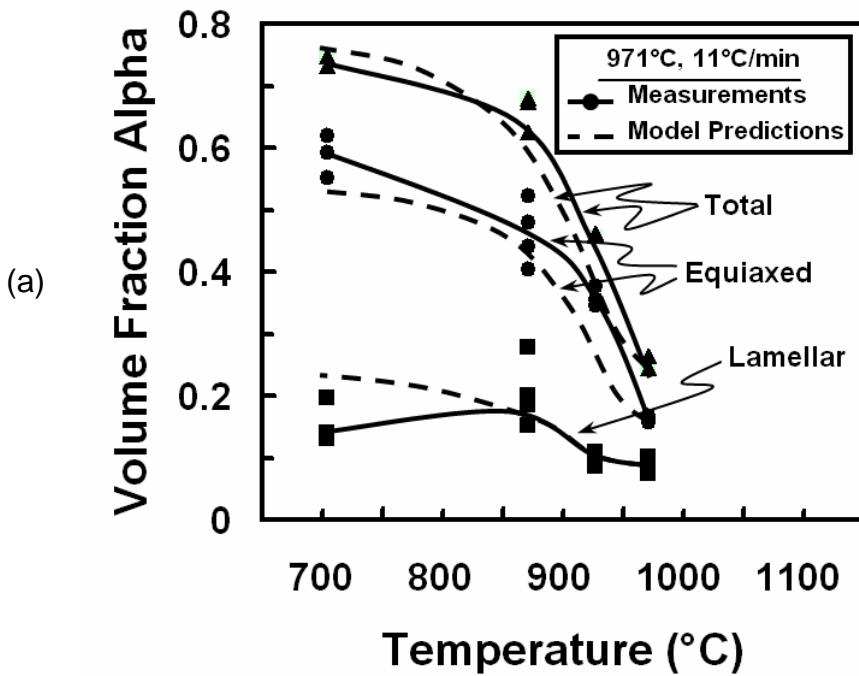


Figure 7. Measured variation of the volume fraction of primary equiaxed, lamellar, and total alpha as a function of temperature during cooling from $T_p = 971^\circ\text{C}$ at a rate of (a) $11^\circ\text{C}/\text{min}$ or (b) $42^\circ\text{C}/\text{min}$. The measurements (data points, solid lines) are compared to model predictions using the decoupled-solution approach (broken lines).

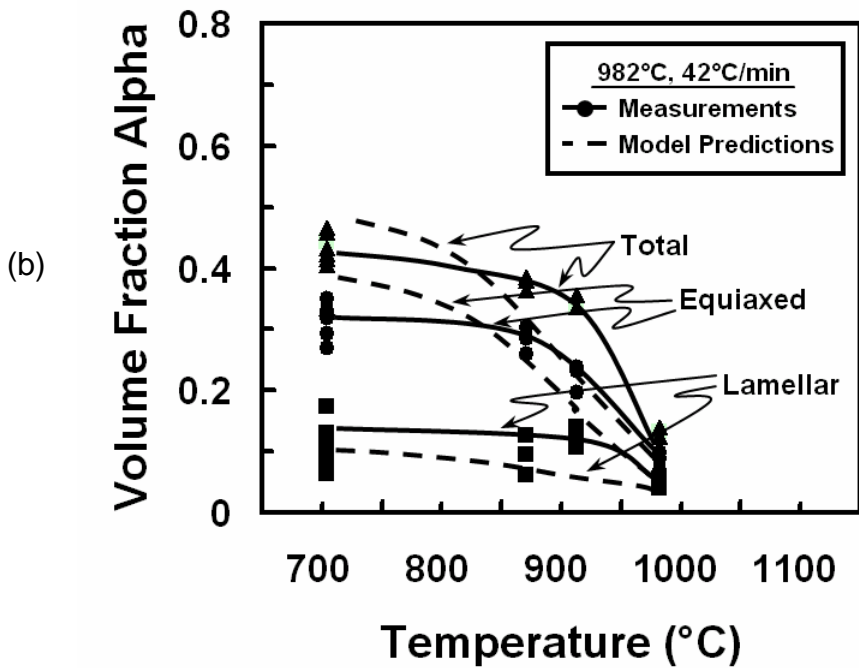
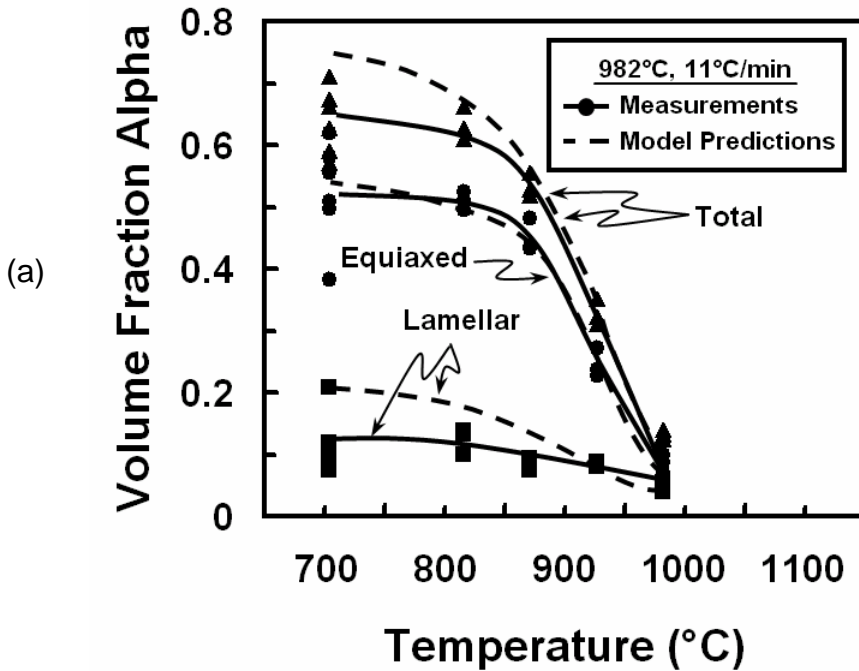


Figure 8. Measured variation of the volume fraction of primary equiaxed, lamellar, and total alpha as a function of temperature during cooling from $T_p = 982^\circ\text{C}$ at a rate of (a) $11^\circ\text{C}/\text{min}$ or (b) $42^\circ\text{C}/\text{min}$. The measurements (data points, solid lines) are compared to model predictions using the decoupled-solution approach (broken lines).

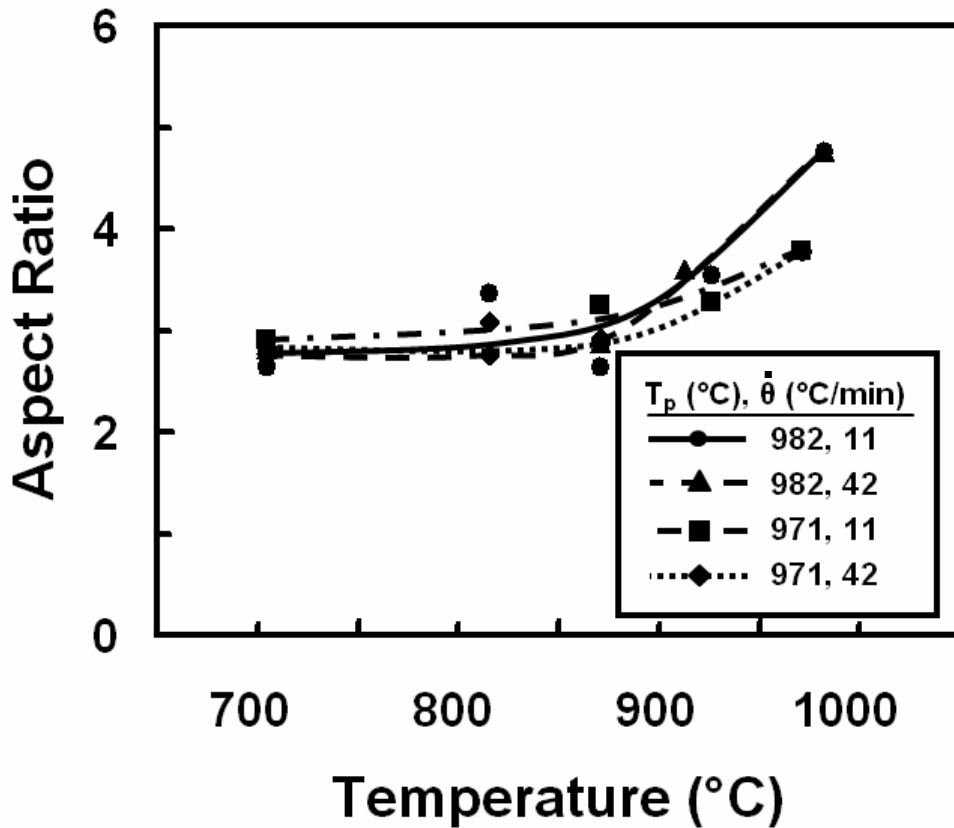


Figure 9. Dependence of aspect (length:thickness) ratio on temperature for remnant alpha lamellae in Ti6242Si during cooling following solution heat treatment.

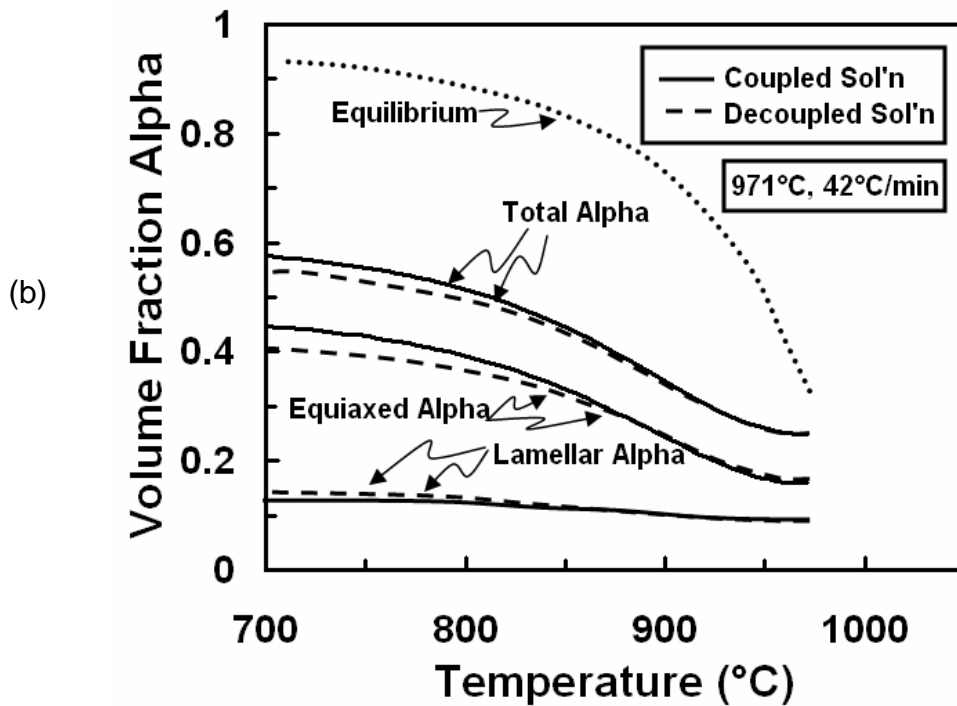
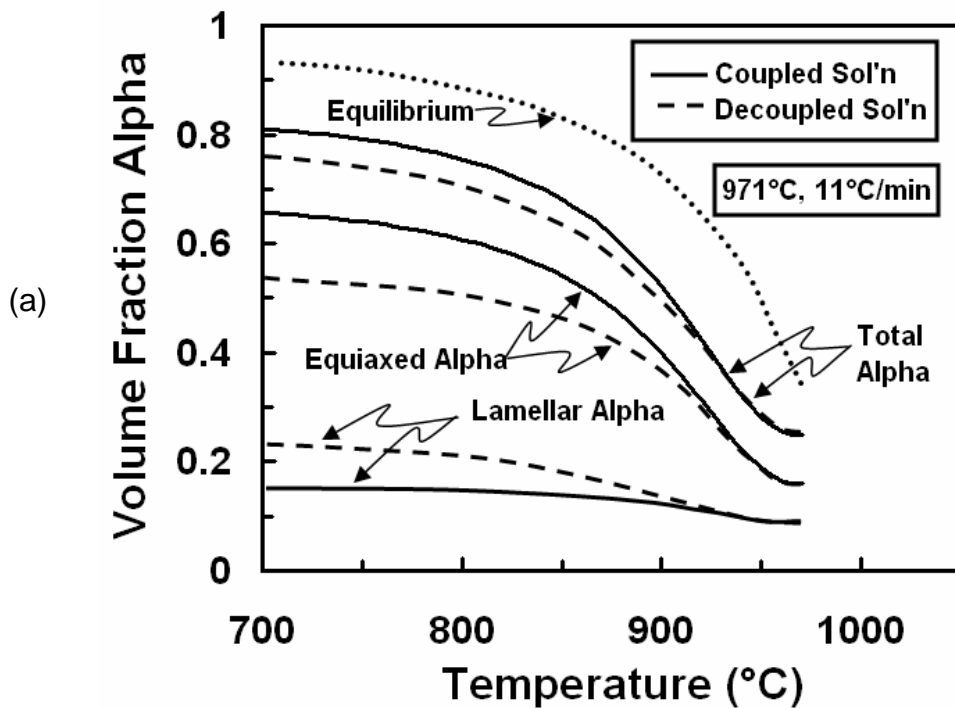


Figure 10. Model predictions of the volume fraction of primary alpha as a function of temperature during cooling from a peak temperature equal to 971°C at a rate of (a) 11°C/min or (b) 42°C/min.

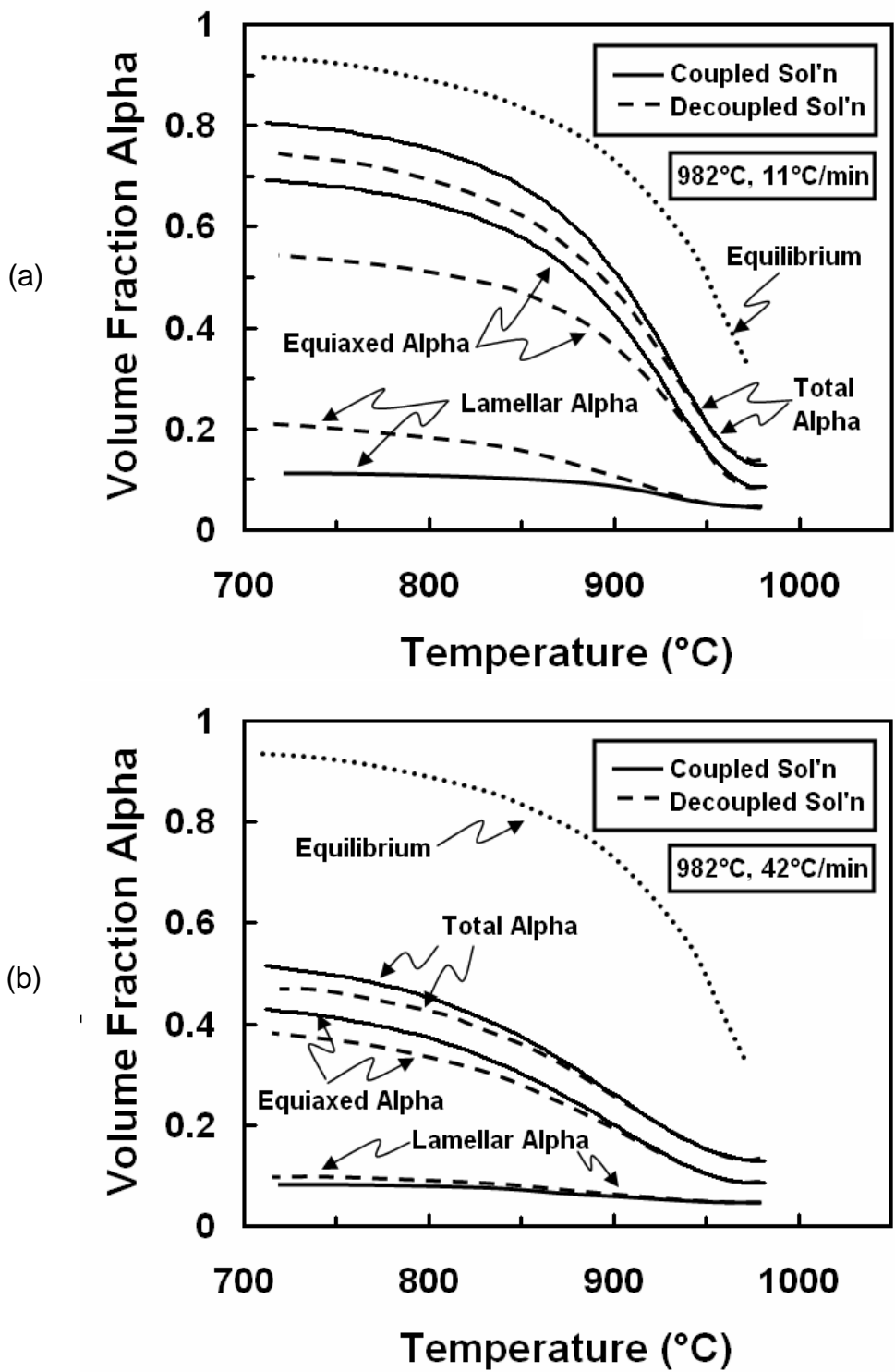


Figure 11. Model predictions of the volume fraction of primary alpha as a function of temperature during cooling from a peak temperature equal to 982°C at a rate of (a) 11°C/min or (b) 42°C/min.

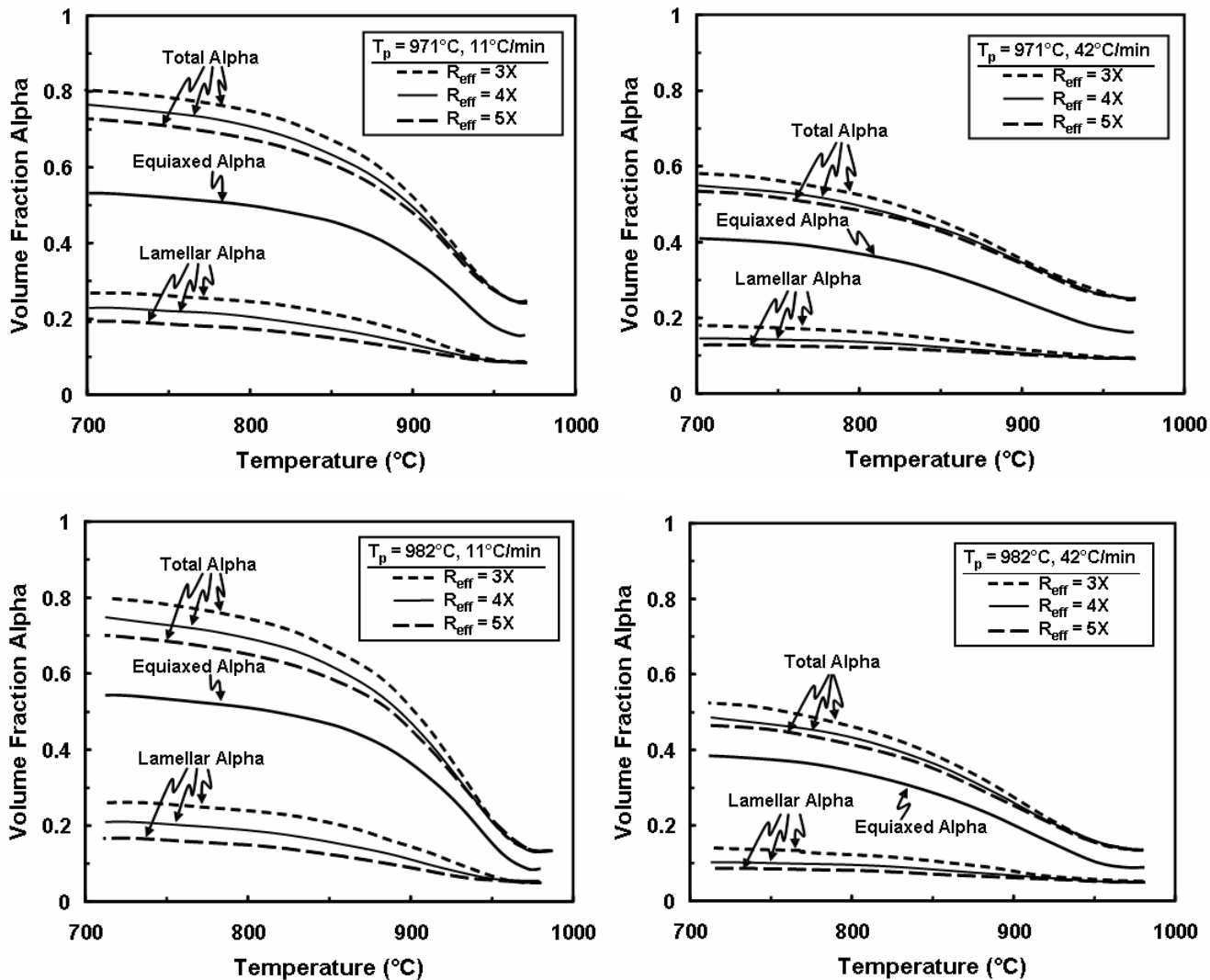


Figure 12. Sensitivity analysis for the growth kinetics of primary alpha assuming $R_{eff} = 3X$, $4X$, or $5X$ for the two peak temperatures and two cooling rates.

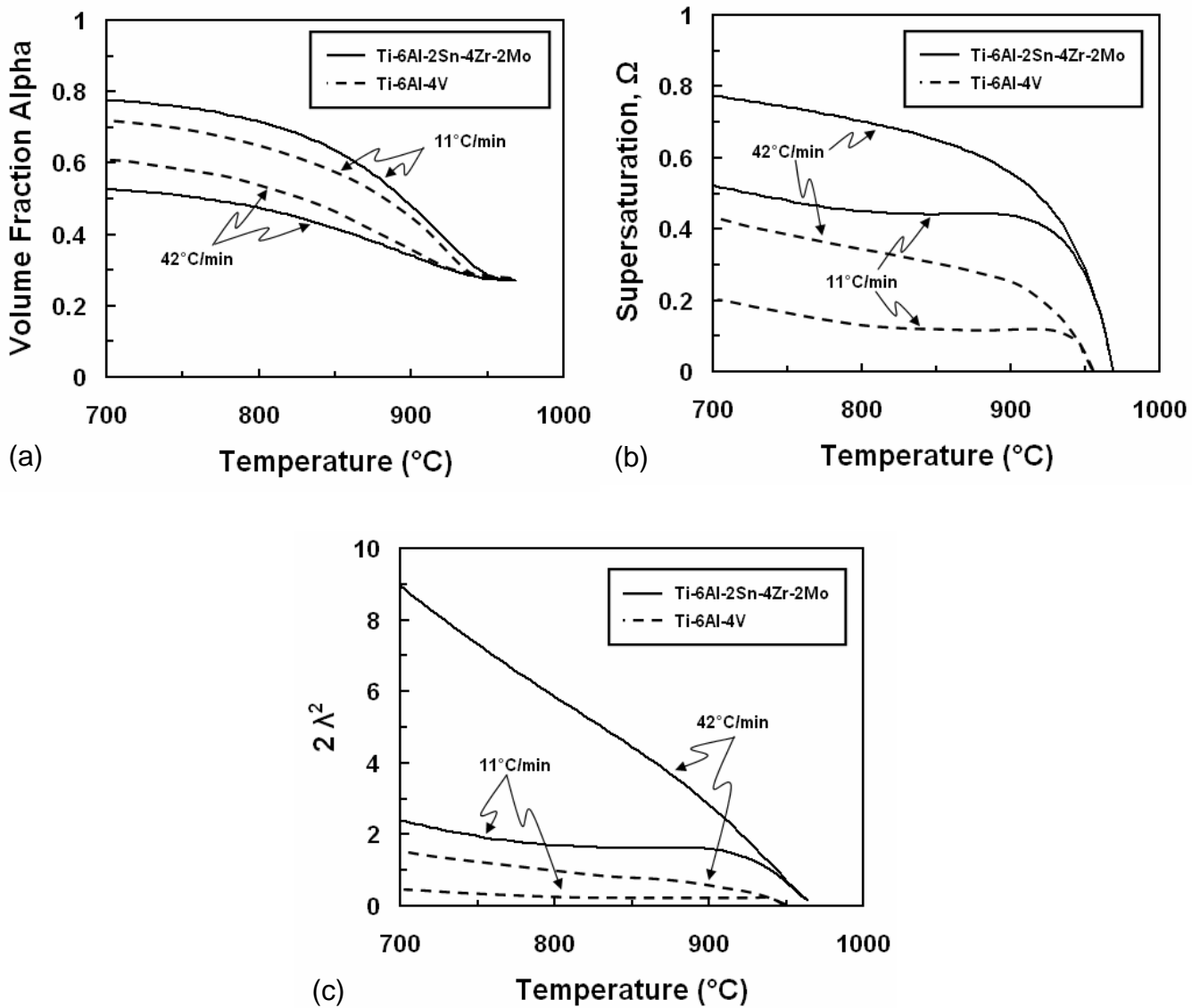


Figure 13. Comparison of model calculations for the heat-treatment response of Ti6242Si and Ti64, each having an equiaxed microstructure with an alpha particle radius of 4 μm and alpha volume fraction of 0.27 at T_p , cooled at either 11 or 42°C/min: (a) Volume fraction of alpha, (b) supersaturation Ω , and (c) λ^2 .